ON A PROPERTY OF THE ZERO-VELOCITY CURVES IN THE REGULAR POLYGON PROBLEM OF $N+1$ BODIES WITH A QUASI-HOMOGENEOUS POTENTIAL

DEMETRIOS GN.FAKIS, TILEMAHOS J. KALVOURIDIS

Department of Mechanics, Faculty of Applied Sciences
National Technical University of Athens
5, Heroes of Polytechnion ave., 157 73, Athens, Greece
Email: fakisdim@gmail.com; tkalvouridis@gmail.com

Abstract. The present study discusses a property of the zero-velocity curves which characterizes the planar motion of a particle in a ring-type $(N+1)$–body system where the central primary creates a Manev-type quasi-homogeneous potential field. This type of potential is often used to describe either the radiating properties or the non-sphericity of a body. The proposed configuration is characterized by three parameters which appear in the equations of motion of the particle in a synodic coordinate frame. Two of these parameters concern the central body with the non-Newtonian potential. When the planar motion of the particle on the plane of the primaries is considered, it is very important to locate the areas of the plane where this motion is permitted. To do this we use an existing Jacobian-type integral of motion and the diagrams $x - C$ (where C is the Jacobian constant), obtained from it. In these diagrams the limiting curves between the permitted and the non-permitted areas of particle motion are the zero-velocity curves. By varying one of the parameters associated with the central primary and keeping the other parameter constant, we have found that the aforementioned curves have common intersection points. We call these points focal and the curves which they belong to, focal curves. We first prove their existence and we provide relations for the exact computation of their coordinates. Then, we deal with the parametric variation of these points and curves and explain the mechanism of their evolution. The results obtained so far are depicted in a number of diagrams, plots and figures.

Key words: $(N+1)-$body ring systems, properties of zero-velocity curves, focal points and curves.

1. INTRODUCTION

The N-body problem has been the subject of a continuous study by Astronomers since the age of Newton and has frequently inspired researchers to develop new models with $N > 3$. One of the problems which falls into this category is the so-called restricted N-body regular polygon problem (or Maxwell-type configuration), where $\nu = N - 1$ of the bodies-members of the system are spherical, homogeneous with equal masses m, and are located at the vertices of an imaginary regular ν-gon, while the Nth body has a different mass m_0 and is located at the center of mass of the system. Elmabsout & Mioc (2001) and Bang & Elmabsout (2004) studied the relative

equilibrium of such formations, while Salo & Yoder (1988), and Vanderbei & Kolemen (2007) proved that this configuration may exist if $\nu \geq 2$, but it may be linearly stable if $\nu > 6$. An interesting case based on the previous configuration is one, where we consider the motion of a small body, natural or artificial, in the vicinity of such a system under the influence of all the primaries. At this point it is worth mentioning some of the studies published over the last 20 years; Sheeres, 1992; Sheeres & Vinh, 1993; Kalvouridis, 1999, 2008; Hadjifotinou & Kalvouridis, 2005; Croustalloudi & Kalvouridis, 2007; Barrio et al., 2008; Papadakis, 2009; Barrabes *et al.* , 2010; etc. During the investigation of the particle dynamics in the Newtonian field of a Maxwell's type regular polygon formation of N massive bodies, one of the present authors (Kalvouridis, 2004) has discovered and proved the existence of a new property that characterizes the zero-velocity curves in the $x - C$ diagrams for the planar motion of the small body. When these curves are drawn for various values of the mass parameter β (ratio of the central mass m_0 to the mass m of a peripheral body), then the parts of these curves which evolve on both sides of the central primary and form a "chimney"-like channel, have two common points. In other words, the bunch of these superposed curves seems to pass through two intersection points which are referred to as focal points.

In this paper we describe a more general version of the problem, by considering that the central body P_0 creates a Manev-type potential which has the form $V = -GMm(A/r + B/r^2)$, This expression strongly resembles the one proposed by Newton himself in a less well-known Corollary of his famous Philosophiae Naturalis Principia Mathematica (Book I, Article IX, Proposition XLIV, Theorem XIV, Corollary 2) (see Mioc & Stavinschi, 1999; Haranas *et al.* , 2011). Newton tried to explain the motion of the apsidal line of the moon, while Manev tried to explain in a classical manner the advance of Mercury's perihelion. Manev published four works concerning this subject between 1924 and 1930 (Maneff, 1924, 1925, 1930a and b). Here, we note that the term "Manev potential" was proposed by Diacu (Delgado *et al.* , 1996) to describe potentials of this type. He also extended this concept to a more general class of potentials that are called "quasi-homogeneous potentials" (Diacu, 1996). Some aspects of the version of the ring problem of $N + 1$ bodies with a central body creating a Manev-type potential field have recently been studied (Arribas & Elipe, 2004; Elipe *et al.* , 2007; Fakis & Kalvouridis, 2013; etc.) and have been used to describe either the non-sphericity of the particular body or its radiating properties. In this work we use the same model of $(N + 1)-$bodies by considering that $A = 1$ and $B = e\alpha$, where α is the side of the regular polygon formation of the primaries and e is Manev's parameter. Thus, the original problem becomes a tri-parametric one and new properties concerning the zero-velocity curves and surfaces arise, as we shall describe in the subsequent paragraphs.

2. EQUATIONS AND INTEGRAL OF PARTICLE MOTION

In order to formulate the problem, we use an inertial Cartesian coordinate system $O\xi\eta\zeta$ located at the central primary P_0 and a synodic coordinate system $Oxyz$, which is rigidly attached to the primaries. The planes $O\xi\eta$ and Oxy coincide with the plane of the primaries (Figure 1). We furthermore assume that the primaries are in relative equilibrium and rotate about Oz axis with constant angular velocity ω here taken as unity.

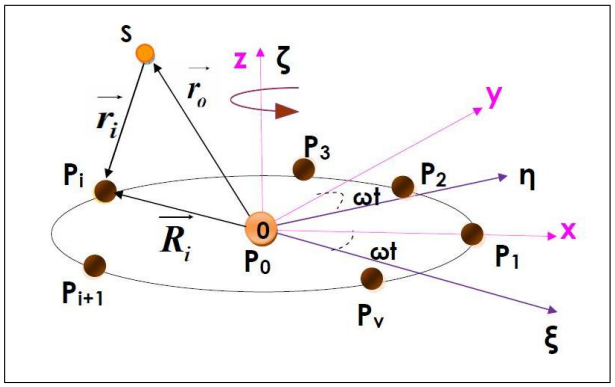

Fig. 1 – The ring configuration of the $(N+1)$ bodies and the two coordinate systems; the inertial $O\xi\eta\zeta$ and the synodic one $Oxyz$. P_i, $i = 0, 1, ..., \nu$ are the primaries and S the small body.

After normalization of the physical quantities, we obtain the following dimensionless second order differential equations which describe the motion of the particle (for a detailed analysis of the whole procedure see Fakis & Kalvouridis, 2013).

$$\begin{aligned} \ddot{x} - 2\dot{y} &= \frac{\partial U}{\partial x} = U_x \\ \ddot{y} + 2\dot{x} &= \frac{\partial U}{\partial y} = U_y \\ \ddot{z} &= \frac{\partial U}{\partial z} = U_z \end{aligned} \tag{1}$$

where

$$U(x,y,z) = \frac{1}{2}\left(x^2+y^2\right) + \frac{1}{\Delta}\left[\beta\left(\frac{1}{r_0} + \frac{e}{r_0^2}\right) + \sum_{i=1}^{\nu}\frac{1}{r_i}\right] \tag{2}$$

and

$$r_0 = \left(x^2+y^2+z^2\right)^{1/2}, \quad r_i = \left[(x_i-x)^2 + (y_i-y)^2 + z^2\right]^{1/2}$$

are the distances of the particle from the central and the peripheral primaries respectively. Also,

$$\Delta = M(\Lambda + \beta M^2 + 2\beta e M^3) \tag{3}$$
$$\Lambda = \sum_{i=2}^{\nu} \frac{\sin^2(\pi/\nu)}{\sin[(i-1)(\pi/\nu)]}, \quad M = 2\sin(\pi/\nu)$$

There is a Jacobian-type integral of motion,

$$\dot{x}^2 + \dot{y}^2 + \dot{z}^2 = 2U(x,y,z) - C \tag{4}$$

which for the planar motion of the particle ($z = 0$, $\dot{z} = 0$) takes the simpler form

$$\dot{x}^2 + \dot{y}^2 = 2U(x,y) - C \tag{5}$$

As we have mentioned before, the problem is characterized by three parameters; the number ν of the peripheral primaries which takes positive integer values, the mass parameter $\beta = m_0/m$ which takes real positive values and parameter e which takes real values either positive or negative. Since quantity Δ is always positive, the negative values of e must satisfy the condition (see Fakis & Kalvouridis, 2013),

$$e > -\frac{\Lambda + \beta M^2}{2\beta M^3} \tag{6}$$

3. ZERO-VELOCITY CURVES AND SURFACES

When particle motion is described in the synodic system $Oxyz$ and we consider planar motions on the xy-plane, the zero-velocity curves which are drawn by using relation (5), separate the regions of the plane where particle motion is permitted from those where this motion is impossible. As it is known, these curves are also isoenergetic, equipotential and isotach. For a given value of the Jacobian constant C, they generally consist of more than one branches, open or closed. If we consider a third dimension that counts the Jacobian constant C, then we obtain the so-called zero-velocity surface. Figure 2a shows such a surface drawn for a configuration with $\nu = 7$ and $e > 0$. In the same figure, the permitted and non-permitted areas of motion are depicted by means of the zero-velocity curves obtained by projecting on the xy-plane various sections of the surface with planes $C = C_a$. Furthermore, the section of this surface with a plane $y = y_c$ creates a diagram, the curves of which are also called zero-velocity curves (Figure 2b). In Figure 2c we see the form of a zero-velocity

surface drawn for negative values of e. We observe that in this case, a folding of the central "chimney" towards its interior is formed (see the detail in Figure 2d).

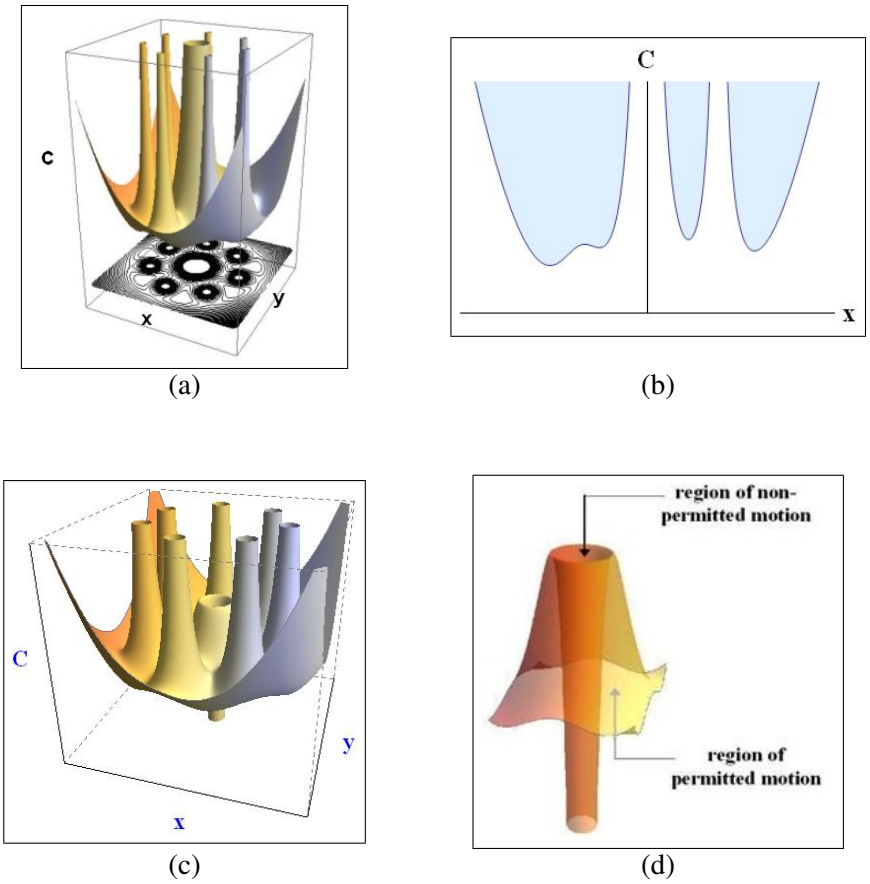

Fig. 2 – Zero-velocity surfaces and (x, C) diagrams for $\nu = 7$, $y = 0$. (a) and (b) $e \geq 0$, (c) and (d) $e < 0$.

4. ON THE EXISTENCE OF FOCAL POINTS AND FOCAL CURVES

4.1. DEFINITIONS AND PRELIMINARY REMARKS

For a given ν and by keeping one of the remaining two parameters, β or e constant, we use the term "focal" points to denote the existing common intersection points of all curves of (5) drawn for various values of the third parameter. This means that the focal points are of two kinds; those obtained by keeping β constant and by varying parameter e and those obtained by keeping e constant and by varying the

mass parameter β. In any case, we symbolize with k' the focal points of the zero-velocity curves drawn for $y = 0$, which are located on the directions of the bisectors of the angles formed by the central primary and two successive peripheral primaries (triangular focal points), and with k the focal points that are located on the radii which connect the central primary to a peripheral one (collinear focal points) (Figures 3a and 3b). By examining the $x - C$ diagrams drawn for $y = 0$ we find:

- Two focal points, one collinear (k-point) and one triangular (k'-point) with different coordinates (x_k, C_k) and $(x_{k'}, C_{k'})$ respectively, when ν is odd, (Figure 3a) and

- Two collinear (k-points) on the same diagram when ν is even (Figure 3b).

Evidently, the distribution of the k and k' points in the xy plane is symmetric in rotations through an angle $2\pi/\nu$ about an axis perpendicular to the Oxy plane passing through the center of mass O preserving in this way the symmetry of the geometric configuration and of the resulting force field.

Here we note that focal points also appear in the $x - C$ diagrams drawn for properly selected non-zero values of y. However, a distinct symbol is not attributed to these points. The reason is that k and k', as can be seen in Figures 3a and 3b, relate to the maxima and minima of the focal curves as we shall describe later.

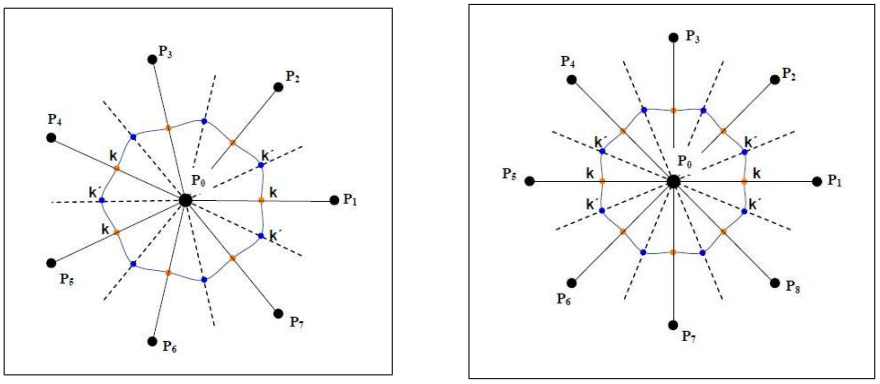

(a) (b)

Fig. 3 – Distribution of k and k' focal points in a regular polygon configuration when: (a) ν is odd, (b) ν is even.

4.2. DETERMINATION OF THE FOCAL POINTS IN THE CASE WHERE β IS CONSTANT AND e VARIES. THE FUNCTION F_β

Let us assume that for a particular configuration ν we have $\beta = \beta'$ and $e \neq e'$. Let us also assume that the respective $C = 2U(x, y = y_c; \beta, e)$ and $C' = 2U'(x, y = y_c; \beta, e')$ curves have an intersection point. In these expressions, the values of y_c are properly chosen so that the plane $y = y_c$ has at least one common point with the zero-velocity surface which evolves around the central primary. Then at the intersection point it must be,

$$2U(x, y = y_c; \beta, e) - C = 2U'(x', y = y_c; \beta, e') - C'$$

and

$$C = C', \quad r_0 = r_0' \neq 0, \quad r_i = r_i'$$

Then,

$$r_0^2 + \frac{2}{\Delta}\left[\beta\left(\frac{1}{r_0} + \frac{e}{r_0^2}\right) + \sum_{i=1}^{\nu}\frac{1}{r_i}\right] = r_0'^2 + \frac{2}{\Delta'}\left[\beta\left(\frac{1}{r_0'} + \frac{e'}{r_0'^2}\right) + \sum_{i=1}^{\nu}\frac{1}{r_i'}\right]$$

and because of (6),

$$\Delta' = \left[\beta\left(\frac{1}{r_0} + \frac{e}{r_0^2}\right) + \sum_{i=1}^{\nu}\frac{1}{r_i}\right] - \Delta\left[\beta\left(\frac{1}{r_0} + \frac{e'}{r_0^2}\right) + \sum_{i=1}^{\nu}\frac{1}{r_i}\right] = 0$$

or

$$\left(\Delta' - \Delta\right)\left[\frac{\beta}{r_0} + \sum_{i=1}^{\nu}\frac{1}{r_i}\right] + \frac{\beta}{r_0^2}\left(\Delta' e - \Delta e'\right) = 0 \tag{7}$$

It is also the case that,

$$\Delta' e - \Delta e' = \left(e - e'\right) M\left(\Lambda + \beta M^2\right) \quad \text{and} \quad \Delta' - \Delta = 2\beta\left(e' - e\right) M^4$$

By replacing into (7) we have

$$\left(e' - e\right)\left[2\beta M^3\left(\frac{\beta}{r_0} + \sum_{i=1}^{\nu}\frac{1}{r_i}\right) - \left(\Lambda + \beta M^2\right)\frac{\beta}{r_0^2}\right] = 0$$

On the assumptions that $e - e' \neq 0$, $r_0 \neq 0$, then at an intersection point the following equation must be satisfied,

$$\sum_{i=1}^{\nu} \frac{1}{r_i} = \frac{(\Lambda + \beta M^2)}{2M^3} \frac{1}{r_0^2} - \frac{\beta}{r_0} \tag{8}$$

or

$$F_\beta = \frac{r_0^2}{K - r_0 \beta} \sum_{i=1}^{\nu} \frac{1}{r_i} - 1 = 0 \tag{9}$$

where

$$K = \frac{\Lambda + \beta M^2}{2M^3}$$

We note that:

- Relation (9) does not depend on e and the focal points are the non-zero roots of (9).
- By replacing each root of (9) in (5) we compute the corresponding value of the Jacobian constant C.
- The locus of all these points obtained for various values of $y = y_c$ is a continuous curve in the (x, y_c, C) space, which is located on the zero-velocity surface and is called focal curve (Figure 4).

4.3. DETERMINATION OF THE FOCAL POINTS IN THE CASE WHERE e IS CONSTANT AND β VARIES. THE FUNCTION F_e

We now suppose that two zero-velocity curves with parameters β, e and β', e, respectively, intersect. Then by assuming that $r_0 \neq 0$ and by following the same procedure as in the previous paragraph 4.2 we obtain after some trivial calculations,

$$\Lambda \left(\frac{1}{r_0} + \frac{e}{r_0^2} \right) - M^2 (1 + 2eM) \sum_{i=1}^{\nu} \frac{1}{r_i'} = 0 \tag{10}$$

or

$$F_e = \frac{M^2 (1 + 2eM}{\Lambda} \left(\frac{r_0^2}{r_0 + e} \right) \sum_{i=1}^{\nu} \frac{1}{r_i} - 1 = 0 \tag{11}$$

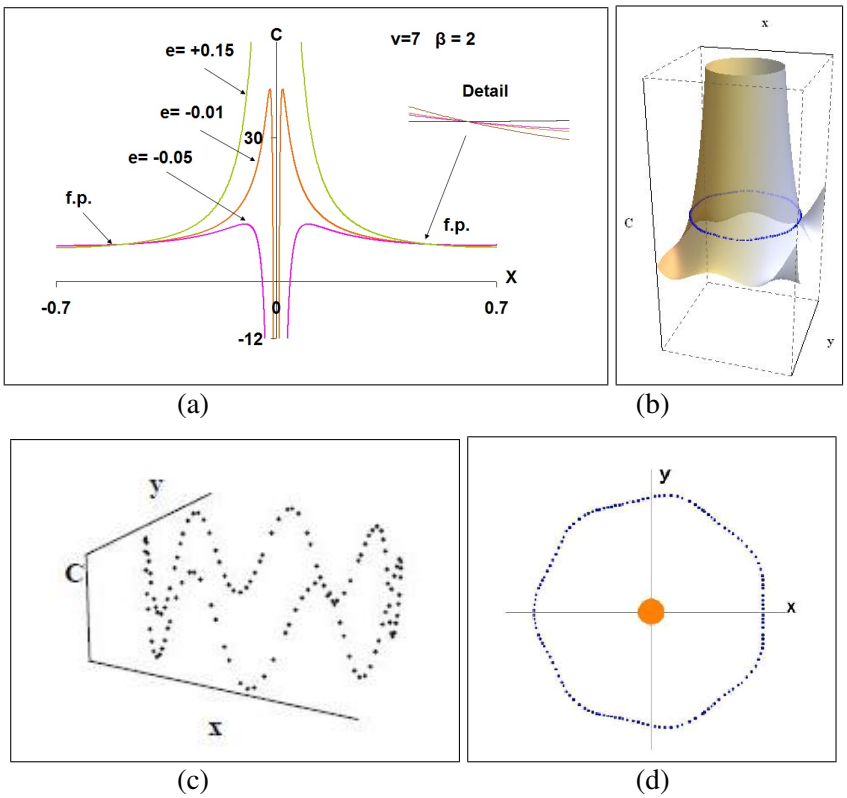

Fig. 4 – (a) Focal points of diagrams $x-C$ for $y=0$, for the case $\nu=7$, $\beta=2$ and various values of e, (b) the focal curve around the central part of the zero-velocity surface, (c) the wavy form of the focal curve, (d) projection of the focal curve on the $xy-$plane.

Relation (11) does not depend on β. This means that, all curves drawn for various values of β will cross a common point (focal point). We consider the following cases:

(i) Case where $e>0$

If $e>0$ two focal points occur by superposing the zero-velocity curves in the $x-C$ diagram for $y=0$ as we have already found in the pure gravitational case. When ν is odd, the coordinates of these points in the $x-C$ diagram are not the same. On the contrary, if ν is even, the two intersection points are symmetric with respect to the $C-$axis, while their Jacobian constants are the same. In Figure 5a we display the $x-C$ diagram obtained for $\nu=7$, $y=0$, $e=+0.05$ and $\beta=2,10,20$ while Figure 5b shows the two existing roots of F_e.

(ii) Case where $e<0$

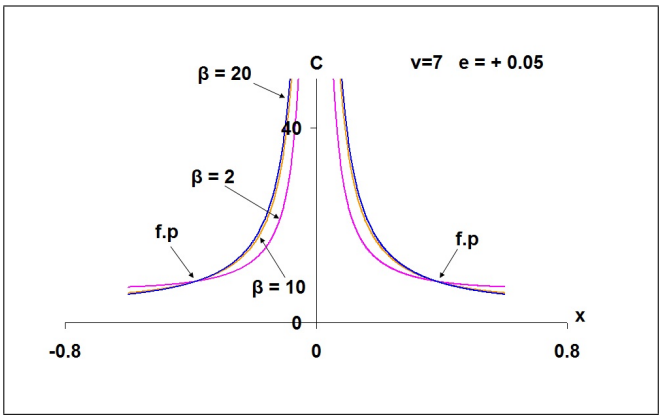

(a)

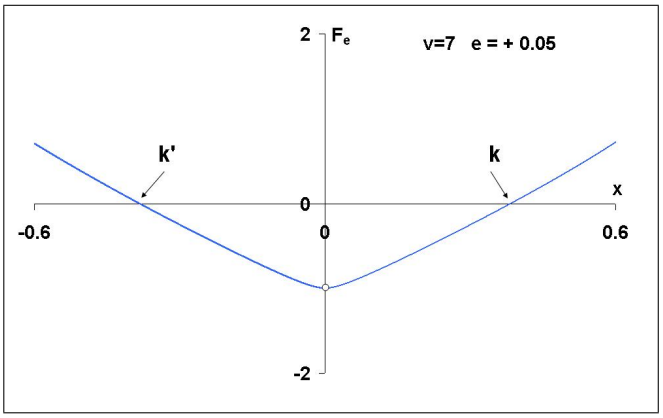

(b)

Fig. 5 – (a) Focal points for $\nu = 7$, $y = 0$, $e = 0.05$ and various values of β, (b) the respective $x - F_e$ diagram with the two roots of F_e.

When $e < 0$, significant changes occur in the zero-velocity surfaces and the $x - C$ diagrams in the vicinity of the central primary which creates a Manev-type potential. Because of the "folding" of the central "chimney", the $x - C$ diagrams may have four, three, two, one or null focal points depending on the values of e. As a consequence, the plots of function F_e for a particular value $y = y_c$, may have four, three, two, one or null zeroes respectively.

In Figure 6 we present several $x - C$ diagrams for various negative values of e and various mass parameters β when $y = 0$ and $\nu = 7$. For very small absolute values of e there are four focal points; two on the left side of the diagram (negative values of x) and two on the right side (positive values of x) (Figure 6a). As the absolute value of e increases, the focal points reduce to three; two with

negative and one with positive values of x. At a particular limiting value of e which is approximately $e = -0.11804$ the focal point on the right branch of the diagram (positive values of x) disappears and only the two focal points on the left branch exist (Figure 6b). Finally, at another limit value of $e = -0.11806$, very close to the previous one, the two intersection points on the left side are reduced to one. Beyond this value, there are no focal points (Figure 6c).

Figure 6d is a plot of function F_e versus x for $y = 0$ and various negative values of e.

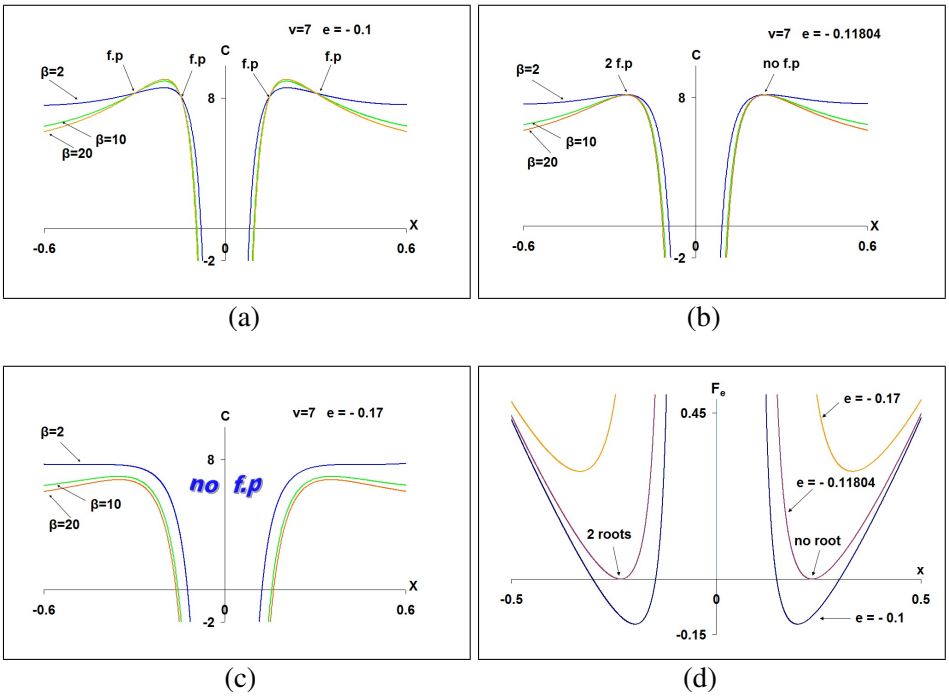

Fig. 6 – Parametric variation of the number of focal points with e. (a) $e = -0.1$, four focal points, (b) $e = -0.11804$ two focal points (left side of the diagram), (c) $e = -0.17$, no focal points, (d) plot of function F_e *versus* x for $y = 0$ and various negative values of e.

As we have mentioned before, the focal points form continuous curves in the (x, y, C) space. Figures 7a and 7b show a case where there are two focal curves, while in Figures 7c and 7d we show their wavy form.

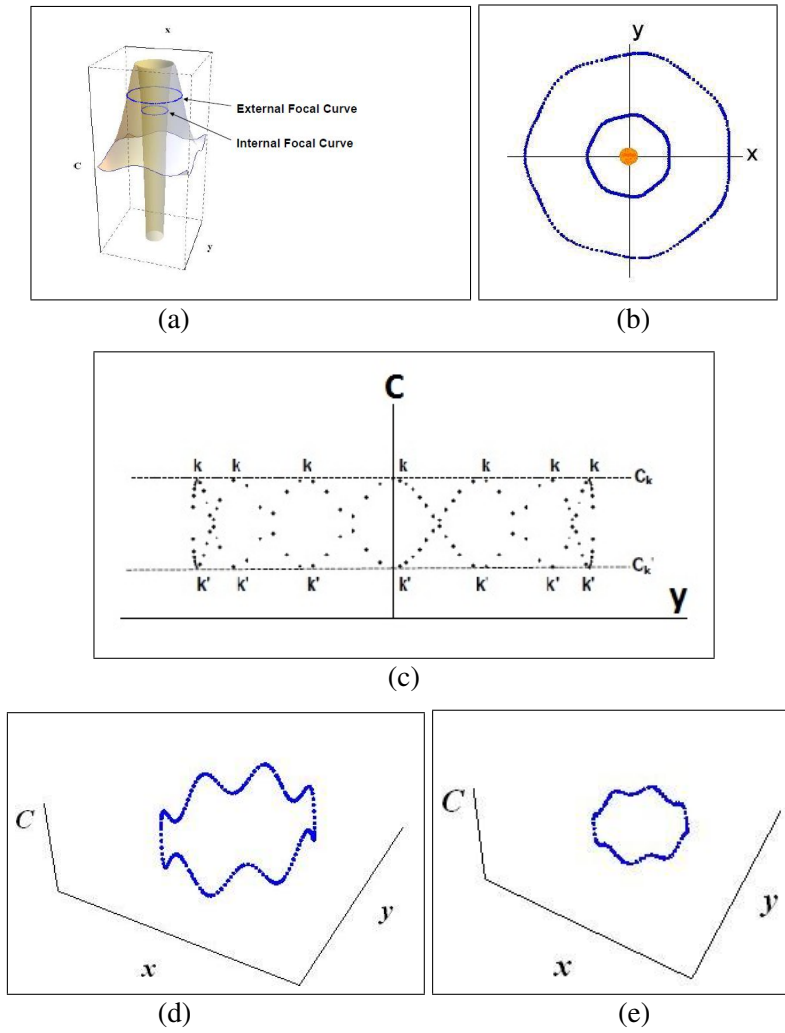

Fig. 7 – A case with two focal curves. (a) focal curves evolving on the central part of the zero-velocity surface, (b) projection of the focal curves on the $xy-$plane, (c) and (d) details of the two wavy focal curves.

5. COMMON INTERSECTION POINTS OF THE FUNCTIONS F_e AND F_β

In addition to the previously mentioned focal points and curves, we have also discovered that when functions F_e and F_β are drawn for $y = 0$ in a common $x - F$ diagram for various values of e and β, they have common intersection points (Figure 8). There are two non-zero such points in this diagram (the common point at $(0, 0)$ must be excluded since we have assumed that $r_0 \neq 0$) which are also focal points. All these points which are obtained for a particular value of ν and for various values

of y, belong to a circle with radius

$$r_0 = \frac{1}{2M}$$

This radius is independent of both e and β and linearly varies with ν. Figure 9 shows the concentric circles which correspond to various values of ν ($\nu = 8, 10, 12, 14, 16, 18$).

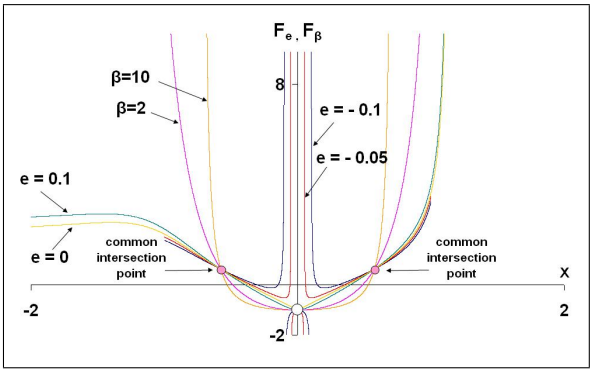

Fig. 8 – Intersection points in a common diagram of functions F_e and F_β for $\nu = 7$, $y = 0$ and various values of parameters e and β.

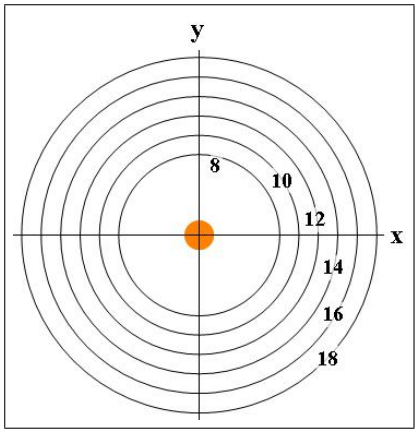

Fig. 9 – Diagram with the loci of the common intersection points of the functions F_e and F_β drawn for various configurations ($\nu = 8, 10, 12, 14, 16, 18$).

6. PARAMETRIC EVOLUTION OF THE $x - C$ DIAGRAMS AND OF THE FOCAL CURVES

6.1. PARAMETRIC VARIATION OF THE $x - C$ DIAGRAMS

(i) Parametric variation with β

Figures 10a and 10b show this variation when $e > 0$ and $e < 0$ respectively for $\nu = 7$.

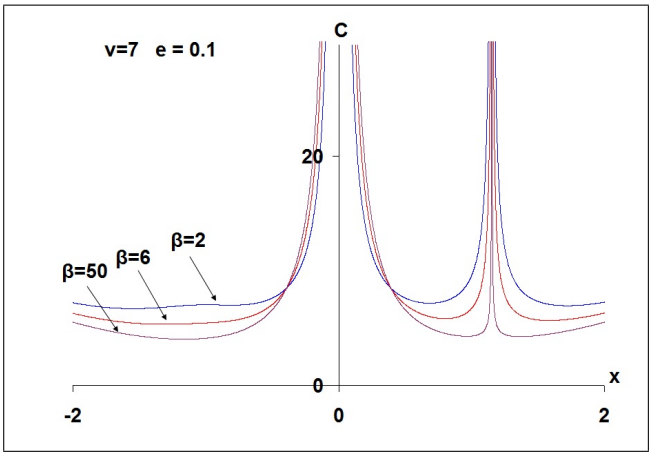

(a)

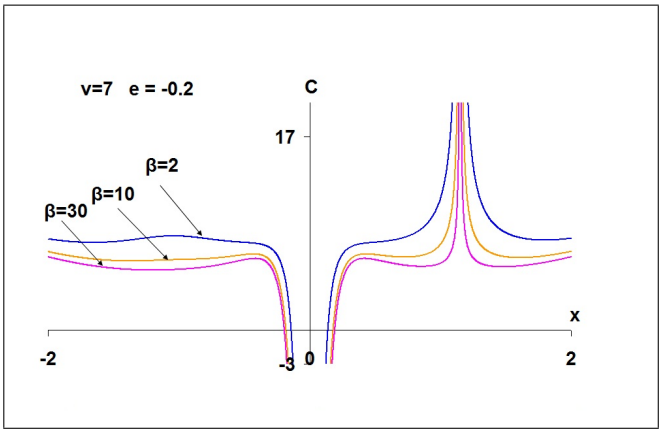

(b)

Fig. 10 – Parametric evolution with β of the zero-velocity curves in the diagrams $x - C$ ($\nu = 7$): (a) $e > 0$ ($e = 0.1$), (b) $e < 0$ ($e = -0.2$).

(ii) Parametric variation with e

Figure 11 shows this variation for $\nu = 7$ and $\beta = 2$ for various values (positive and negative) of e. When $e < 0$ there is a folding of the central part of the diagram towards its interior.

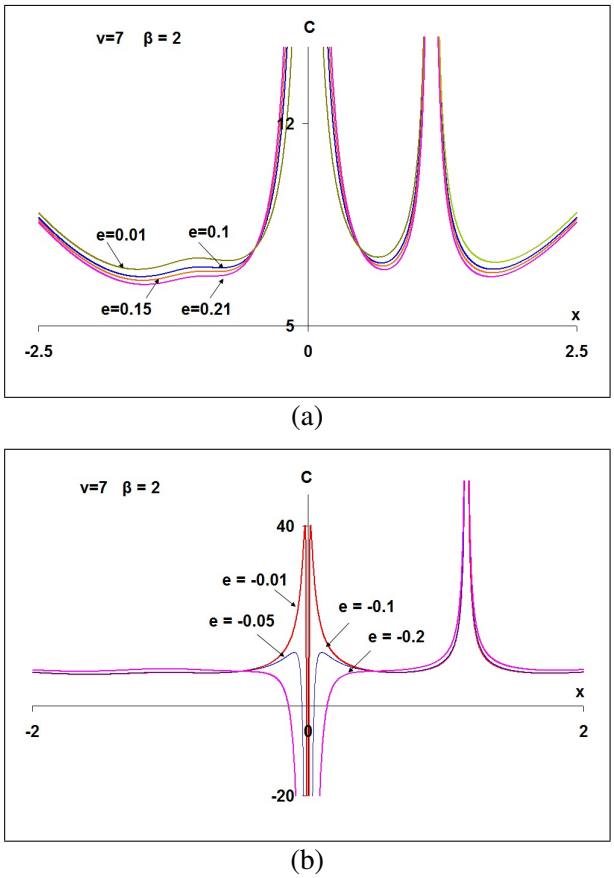

Fig. 11 – Parametric evolution with e of the zero-velocity curves in the diagrams $x - C$ ($\nu = 7$, $\beta = 2$): (a) $e > 0$, (b) $e < 0$).

6.2. PARAMETRIC EVOLUTION OF THE FOCAL CURVES

(i) Case where β is kept constant and e varies (the focal points and the focal curves are independent of e).

By numerical investigation, we have found that the C values of the focal points are bounded between an upper and a lower bound (Figure 12). The former

bound is reached when $\beta \to 0$, while the latter is reached when β increases sufficiently ($\beta > 1000$). For a configuration with $\nu = 7$, these bounds are $C_U \approx 8.621$ and $C_L \approx 5.64$ respectively. At this point we note that these values depend on the number ν of the peripheral primaries.

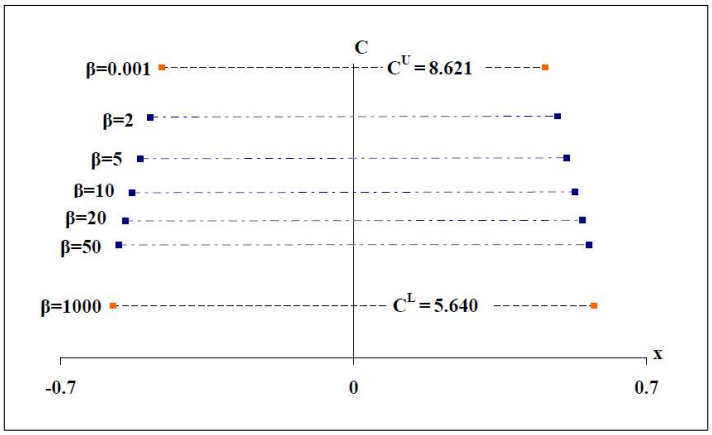

Fig. 12 – A sketch showing in an $x - C$ diagram, the variation of the mean values $C_\mu^\beta = \left(C_k^\beta + C_{k'}^\beta\right)/2$ for $\nu = 7$ and various values of β.

(ii) Case where e is kept constant and β varies (the focal points and the focal curves are independent of β).

We have found that when $e > 0$ the focal curve changes in size and shape as parameters β and ν vary, however it never disappears and never degenerates to a point. On the contrary, if $e < 0$, then the evolution of the focal curves depends on the value of ν. The two diagrams of Figure 13 depict this evolution. More precisely, Figure 13a shows the variation with $e < 0$ of the mean values $x_\mu^e = \left(x_k^e + x_{k'}^e\right)/2$ of the two focal curves (external and internal) for various configurations ν, while Figure 13b shows the respective variation with $e < 0$ of the mean values $C_\mu^e = \left(C_k^e + C_{k'}^e\right)/2$ for various ν. For each ν the upper branch of the curves describes the evolution of the external focal curve, while the lower one describes the evolution of the internal focal curve. In both diagrams (Figures 13, a and b), when $\nu < 25$ the two curves meet at some limiting value e_{lim}. Beyond this value the focal curves no longer exist. In Table 1 we give the values of e_{lim} for various configurations $\nu < 25$ while in Figure 14 we show the mechanism of the evolution of the focal curves in the case where $\nu = 7$. In both Figures 13a, b and 14 we can see that as the absolute value of e increases, the internal focal curve expands and the external curve shrinks. At the same time

the mean values x^e_μ and C^e_μ of the internal focal curve increase, while the ones of the external curve decrease. As a consequence, the two branches approach each other until they meet at the limiting value e_{lim}. However, when $\nu \geq 25$ the situation changes, since the two branches never meet and therefore, the two focal curves exist even for relatively large absolute values of e (Figure 13).

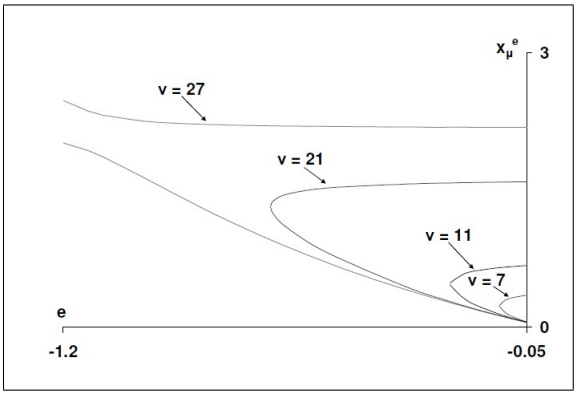

(a)

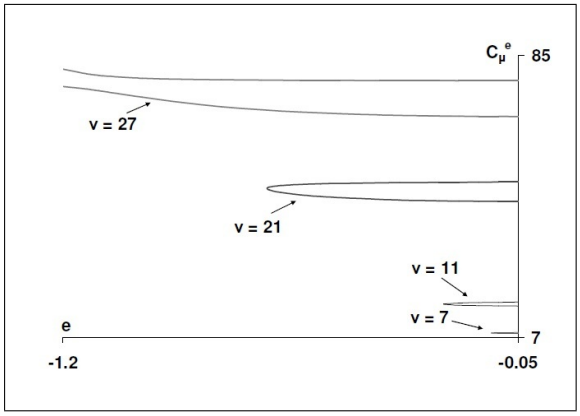

(b)

Fig. 13 – Variation with $e < 0$ of: (a) the mean values $x^e_\mu = \left(x^e_k + x^e_{k'}\right)/2$ and (b) the mean values $C^e_\mu = \left(C^e_k + C^e_{k'}\right)/2$, of the two focal curves for various configurations ν. For each ν the upper branch of the curves describes the evolution of the external curve, while the lower one describes the evolution of the internal focal curve.

Table 1

Critical values e_{lim} for various configurations

ν	$\mathbf{e_{lim}}$
7	-0.11806
8	-0.14551
9	-0.17496
10	-0.20630
11	-0.23951
18	-0.52617
21	-0.6852
24	-0.88665

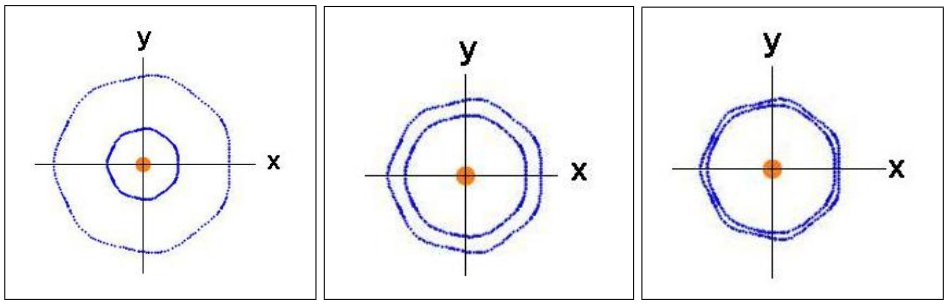

(a) (b) (c)

Fig. 14 – Three different phases of the evolution process of the two focal curves for $\nu = 7$ when e ($e < 0$) varies (a, b, and c). As the absolute value of e increases the two curves approach each other until both disappear.

7. SUMMARY AND GENERAL CONCLUSIONS

We have studied some new properties of the zero-velocity curves and surfaces of a small body in a regular polygon configuration of N bodies, where the central primary creates a Manev-type potential field. These properties concern common intersection points the loci of which are the focal curves. The problem is a tri-parametric one and by considering a particular number ν of the peripheral primaries, the aforementioned properties are influenced by the two remaining parameters, that is, the mass parameter β and Manev's parameter e, especially when the latter takes negative values. We can summarize the main results obtained from our investigation as follows:

- The focal curves are three-dimensional wavy curves in the (x, y, C) space and present the same symmetry as the geometric configuration of the primaries and of the resultant force field (rotations through an angle $2\pi/\nu$ about an axis per-

pendicular to the Oxy plane passing through the center of mass O).

- They appear on the part of the zero-velocity surface which evolves around the central primary, since both parameters β and e are related to the physical properties of this primary.

- Each focal curve has local minima and maxima regarding the Jacobian constant C. The maximum values C_k appear on the radii which connect the central primary to a peripheral one (collinear or $k-$points), while their minimum values $C_{k'}$ appear on the bisectors of the angles formed by the central and two consecutive primaries (triangular or k'-points). The number of k and k' points is equal to the number ν of the peripheral primaries. The absolute differences of the coordinates between the minima and maxima get smaller as ν increases.

- For a particular ν, two kinds of focal curves may exist; (1) those obtained when β is kept constant and parameter e varies (under the restriction of condition (6)) and, (2) those obtained when e is kept constant and the mass parameter β varies. In the first case there is always one focal curve which is the locus of the non zero-roots of a function F_β that is independent of e, while in the latter case the focal points are the non-zero roots of a function F_e which is independent of β. Here we have two sub-cases; if $e \geq 0$ there is only one focal curve which evolves on and around the central part of the zero-velocity surface. However, if $e < 0$, the existing focal curves develop on the external and the internal parts of the zero-velocity surface which surrounds the central primary. Their existence, size and evolution depend on the values of e and ν.

Closing this article we would like to express our intention to apply the above analysis in more complex $N-$body ring-type configurations which will be characterized by several parameters and to study the existence and the evolution of the focal curves, so as to be able to generalize the conclusions obtained so far.

REFERENCES

Arribas, M., Elipe A.: 2004, *Mechan.Res.Comm.* **31**, 1.
Bang, D., Elmabsout, B.: 2004, *Celest. Mech. Dyn. Astron.* **89**, 305.
Barrabes, E., Cors, J.M., Hall, G.R.: 2010, *SIAM Journal on Applied Dynamical Systems* **9**, 634.
Barrio, R., Blesa, F., Serrano, S.: 2008, *Chaos, Solitons and Fractals* **36**, 1067.
Croustalloudi M., Kalvouridis T.: 2007, *Planetary and Space Sci.*, **55**, 53.
Delgado, J., Diacu, F., Lacomba, E.A., Mingarelli, A., Mioc, V., Perez-Chavela, E., Stoica, C.: 1996, *J.Math.Phys.*, **37**, 2748.
Diacu, F.: 1996, *J.Differential Equations*, **128**, 58.
Elipe, A., Arribas, M., Kalvouridis, T.J.: 2007, *Journal of Guidance, Control and Dynamics*, **30**, No.6, 1640.

Elmabsout, B., Mioc, V.: 2001, *Romanian Astron. J.* **11**, 121.
Fakis, D.Gn., Kalvouridis, T.J.: 2013, *Celest.Mech.& Dynam.Astron.* **116**, 229.
Hadjifotinou, K.G., Kalvouridis, T.J.: 2005, *International Journal of Bifurcation and Chaos* **15**, 2681.
Haranas, I., Ragos, O., Mioc, V.: 2011, *Astrophys.Space Sci.* **332**, 107.
Kalvouridis, T. J.: 1999, *Astrophys. Sp.Sci.* **260**, 3, 309.
Kalvouridis, T.J.: 2004, *Planetary and Space Science* **52**, 10, 909.
Kalvouridis, T.J.: 2008, Particle motions in Maxwells ring dynamical systems, *Celest. Mech. Dyn. Astron.* **102**, 191.
Maneff, G.: 1924, La gravitation et le principe de l'action et de la réaction, *C.R. Acad. Sci. Paris*, **178**, 2159-2161.
Maneff, G.: 1925, *Z. Phys.* **31**, 786.
Maneff, G.: 1930a, *C.R. Acad. Sci. Paris* **190**, 963.
Maneff, G.: 1930b, *C.R. Acad. Sci. Paris* **190**, 1374.
Mioc, V., Stavinschi, M.: 1999, *Physica Scripta* **60**, 483.
Elmabsout, B., Mioc, V.: 2001, *Romanian Astron. J.* **11**, 121.
Papadakis, K.E.: 2009, *Astrophys. Space Sci.* **323**, 261.
Salo, H., Yoder, C. F.: 1988, . *Astron. Astrophys.* **205**, 309.
Scheeres, D.: 1992, On symmetric central configurations with application to satellite motion about rings, PhD Thesis, The University of Michigan.
Scheeres, D.J., Vinh, N.X.: 1993, *Acta Astronautica* **29**, No.4, 237.
Vanderbei, R.J., Kolemen, E.:2007, *Astron.J.* **133**, 656.

Received on 28 April 2014